Doubly Fed Induction Machine Drive Hardware Laboratory for Distance Learning Education

Giovanna Oriti, *Senior Member, IEEE*, Alexander L. Julian, *Member, IEEE*, and Daniel Zulaica, *Member, IEEE*

***Abstract*—This paper presents the technology and user interface developed to create a doubly fed induction machine (DFIM) remotely controlled hardware laboratory for DL education. The new laboratory is designed to reinforce the theory learned in class and to verify that modeling and simulations of the laboratory machine are accurate. The power conversion system is controlled by two field-programmable gate array-based controllers which communicate with a web server PC through a USB interface so that the laboratory can be executed on campus as well as remotely. The remote students only need access to a PC with Internet connection and a standard browser, without the need to install any software or modify its security settings. The pedagogical value of this laboratory is reinforced by positive student's feedback.**

***Index Terms*—Doubly fed induction machine (DFIM), distance learning (DL) education, power conversion systems, web-based laboratory, wind power generation systems.**

I. Introduction

WIND power generation systems are widespread, and as the power level of the wind turbines increases, so does the need to control the power flow through power electronic systems. This technology creates the need to educate engineers to design and operate complex power electronics-based systems. As engineering education is now available not only on university campuses but also at the student's own location, thanks to distance learning (DL) courses, educational material and the hardware laboratory experiments need to be accessible through the Internet [1]–[7]. Providing DL students with hardware laboratory experience is challenging from both logistical and pedagogical points of view. Logistically, the hardware needs to be entirely controllable by a computer. The computer must be a web server providing Internet access to the hardware, and finally, the student should not be required to have administrator rights to his/her remote computer in order to access the DL laboratory. From a pedagogical point of view, the remote user interface must be easy to understand and operate. It should also provide a meaningful learning experience to add to the theory and modeling that are part of the regular class work. Although much literature is available on doubly fed induction machine (DFIM) drives [8], [9], including hardware simulators for laboratory experiments [10], [11], to the authors' knowledge a remotely controlled DFIM drive system for DL courses has not been presented to date. The novel contribution of this paper includes the power electronics technology and user interface developed to make a DFIM drive accessible to DL students.

This paper presents a new DL laboratory, which allows the remote student to experimentally verify the operation of a DFIM drive system emulating a wind power turbine, connected to the grid or a bidirectional drive for ship propulsion applications. The DL laboratory provides the students with hardware experience including the ability to change the commanded speed and input torque to the machine, listening in real time to the sounds associated with the different speeds of the DFIM and acquiring the experimental waveforms from the oscilloscope. The DFIM laboratory remote access is made possible by digital electronics that control the hardware and communicate with the Internet via a web server. Field-programmable gate arrays (FPGAs) serve as the digital electronic platform to gather sensor data and control the power electronics hardware. The student design center (SDC) introduced in [3] is used as the basis for the drive's control system; however, the new DL laboratory setup presented in this paper utilizes a USB interface for faster and more flexible data processing capabilities. Additionally, the web interface software has been simplified with respect to the previous version. The remote operator only needs a standard web browser to access the DL laboratory. No administrator rights are required to change security settings or to install any software.

This paper is organized as follows: Section II presents the embedded electronics hardware and software setup for the DFIM drive laboratory. In Section III, the web interface is described, including the Java software and tools utilized to create an effective graphic user interface accessible through a standard web browser. Section IV presents the details of the DFIM drive hardware implementation and operation. In Section V, the machine model and simulations are presented. Section VI presents the contents of the DL laboratory website, including instructions for the students to execute the laboratory assignments. The results of a laboratory session are presented in Section VII, including experimental measurements and comparison to the simulations. The positive results of a student's survey are presented in Section VIII and some conclusions are presented in Section IX.

II. Embedded Electronics Platform to Control the DFIM Drive

Fig. 1 shows the block diagram of the embedded electronics platform, which is referred to as SDC version 2 (SDC2)

Manuscript received December 12, 2012; revised January 25, 2013; accepted March 8, 2013. Date of current version July 18, 2013. Recommended for publication by Associate Editor A. M. Trzynadlowski.

The authors are with the Department of Electrical and Computer Engineering, Naval Postgraduate School, Monterey, CA, 93943 USA (e-mail: giovanna.oriti@ieee.org; alexander.julian@ieee.org; dpzulaic@nps.edu).

Color versions of one or more of the figures in this paper are available online at http://ieeexplore.ieee.org.

Digital Object Identifier 10.1109/TPEL.2013.2252629

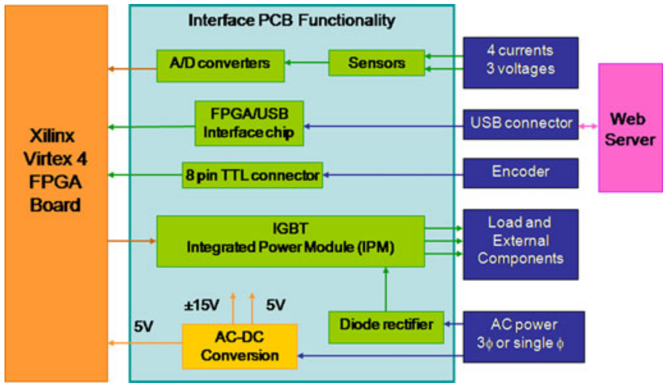

Fig. 1. SDC2 block diagram.

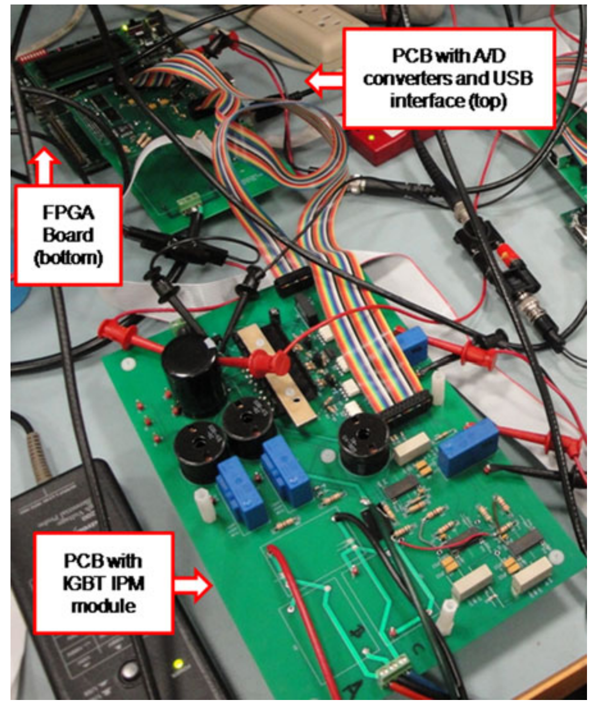

Fig. 2. Photograph of the SDC2 in the laboratory.

hereafter. The SDC2 includes the power electronics and is used to control the DFIM drive and its load. Additionally, the SDC2 connects the DFIM drive to the PC used as web server.

The SDC2 block diagram in Fig. 1 shows a Xilinx Virtex 4 development board [12] on the left. Xilinx provides the software packages together with the development board to speed up the FPGA programming work. The design is carried out using the MATLAB/Simulink software [13] and it is compiled by Xilinx's software to program the FPGA. Therefore, knowledge of VHDL, the hardware description language for very high speed integrated circuits, is not required to design the power converter control system. The large Virtex 4 FPGA chip allows flexibility when experimenting with different power conversion systems and control/modulation strategies. Optimization of the FPGA algorithms, which would reduce the size and cost of the FPGA chip, is not an objective for the purpose of the educational laboratory.

The "interface printed circuit board (PCB) functionality" in Fig. 1 is realized by two custom PCBs, one for the power conversion components and the other for the signal processing components. The photograph in Fig. 2 shows the SDC2 as it is assembled in the laboratory. The PCB with a power converter includes an insulated-gate bipolar transistor (IGBT) integrated power module (IPM), current and voltage sensors, passive components for the dc bus and the output filter, dc power supply. The IGBT IPM includes six diodes and six IGBTs in the standard three-phase three-legs configuration. The second PCB includes a USB interface chip, USB connector to interface with the web server, analog-to-digital converters, voltage level shifters, and several other connectors to interface with the other boards. This PCB is mounted on top of the FPGA board as shown in Fig. 2. The power supply on this board provides power for the power converter board as well. They both can be mounted on top of the PCB with the power converter to create a compact stack, although this is not shown in the photograph.

The DFIM drive described in this paper includes two SDC2 systems, one for the three-phase rectifier and one for the three-phase inverter as described in Section IV. Additionally, a third SDC2 is used to control the dc motor which is the load for the DFIM.

III. Web Publishing

Our approach to deliver the DFIM laboratory to the remote students via the World Wide Web was constrained by the following requirements for the Naval Postgraduate School (NPS) DL program:

1) The DL laboratory must be accessible through a standard web browser so that firewalls are not a problem. Many students will work behind network firewalls that limit the traffic into a network to reduce hacking attempts.
2) The DL laboratory must require no software installation on the remote user's PC. Many students may not have system administrator privileges to download and install client programs. For example, Java applets require the student to have the Java Runtime Environment (JRE) or Java Development Kit (JDK) installed. Another example is the National Instruments LabVIEW client, which students would also need to download and install, in addition to using several different network ports [1], [6], [7].

Given the requirements described previously, we chose to use a Java server application to publish the laboratory interface as a standard web page. A very nice feature of the Java server is that it renders Java code into standard HTML code and serves that to the student's web browser; thus, there is no need to have the JRE or JDK installed on the student's computer. Fig. 3 shows a block diagram showing the technology and our web publishing design. The hardware control panel displayed on the remote user's web browser is presented in Section VII (see Figs. 10 and 12). The control panel includes the ON/OFF button which controls the DFIM and two sliders to set the reference speed and the dc motor armature current, which changes the torque applied to the DFIM, respectively. It also includes real-time readings of

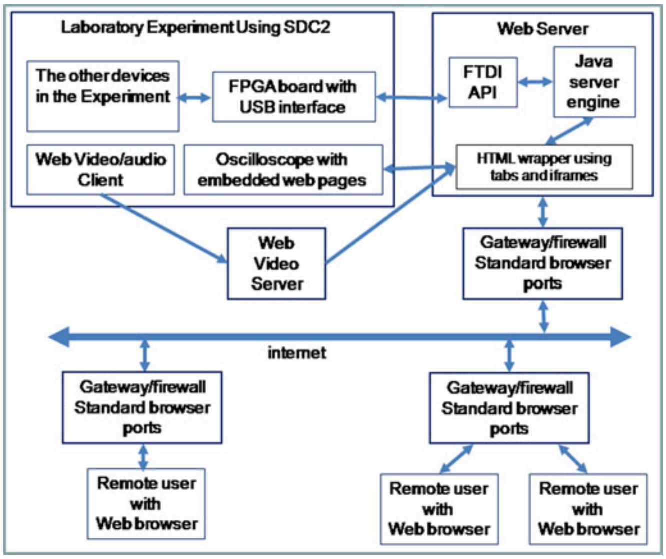

Fig. 3. Block diagram describing the web publishing method.

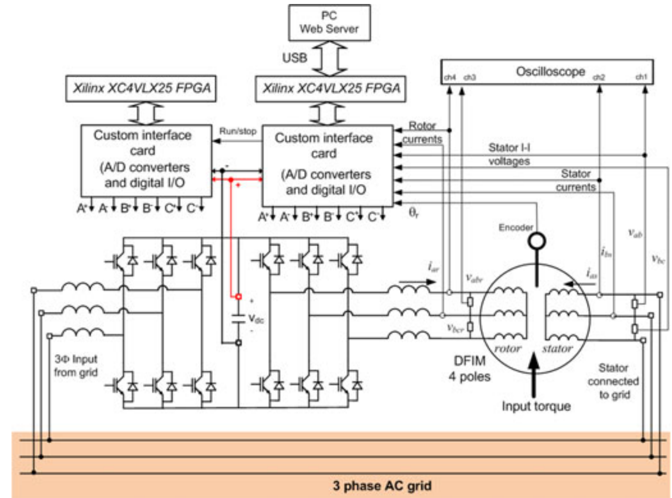

Fig. 4. DFIM drive schematics as implemented in the laboratory.

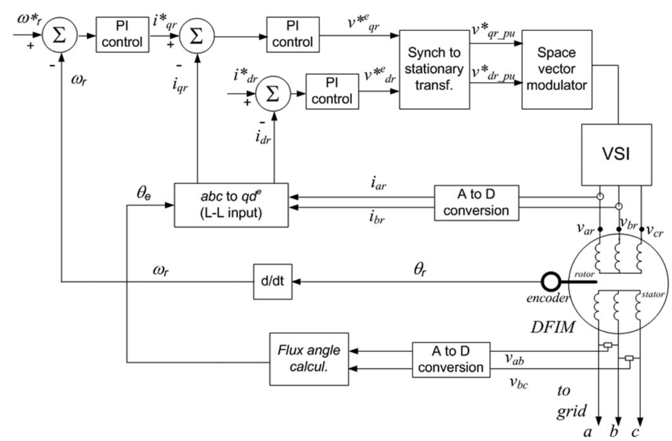

Fig. 5. Rotor-side converter control system.

the power converter's dc-bus voltage, machine speed and power going into DFIM rotor, stator and dc machine.

Several features were desired to enhance the user experience. These features do not need direct Java coding, such as to access an application programming interface library of routines. A simple schematic of the power system electrical flow was desired along with slider options that limit the values sent to the powered device to reduce potential problems that might destroy the hardware. The first user to select the active power button takes control of the experiment. Any other user cannot enter information or start the power button; however, the user can still observe the experiment. When the first user turns off the power button, control can be taken by the observing user. Javascript routines were used to accomplish these tasks. Javascript is available on all standard web browsers.

Standard HTML features allowed us to display on the same page several separate web pages that includes one live streaming video page. The HTML iframe feature allows this. Separate iframes on the same web page independently display embedded web pages.

IV. DFIM Drive Laboratory Architecture

This section describes the hardware architecture that the students access remotely to run the DFIM drive in real time. Fig. 4 shows a schematic of the laboratory setup including the embedded electronics functionality, power converter topology, machine and measuring tools. The DFIM is rated 0.25 hp and its rotor is controlled by a three-phase voltage-source converter as shown in Fig. 4. The stator windings are connected to the grid. This configuration is well known and it is sometimes referred to as Scherbius drive [9]. In this configuration, the power converter is only connected to the rotor circuit; therefore, the drive power electronics need to only manage 25% of the power transferred from the machine to the grid, when operating as a generator [8]. The "input torque" indicated in Fig. 4 is provided by a dc machine which is connected to the DFIM with a rubber belt.

Two SDC2 systems, as described in Section II, are used to implement the two bidirectional three-phase power converters shown in Fig. 4. The full-bridge converter on the left of Fig. 4 is indicated thereafter as a grid-side converter, while the other one is defined as a rotor-side converter because it is connected to the DFIM rotor. The control system of the rotor-side converter is connected to the web server via USB interface for real-time communication. Its four current sensors are used to acquire two stator and two rotor currents as depicted in Fig. 4. An encoder is also used to measure the speed of the DIFM. The grid-side converter communicates with the control system of the rotor-side converter.

Fig. 5 shows a block diagram of the rotor-side converter control algorithm. A speed reference $\omega *_r$ is the controller input which the user can manually schedule from the web interface shown in Fig. 4. The speed proportional-integral (PI) controller defines a reference current that is proportional to the torque. The current PI controller defines the voltage-source inverter output voltage. The voltage-source inverter is controlled using space vector modulation as described in [14]. The grid-side converter

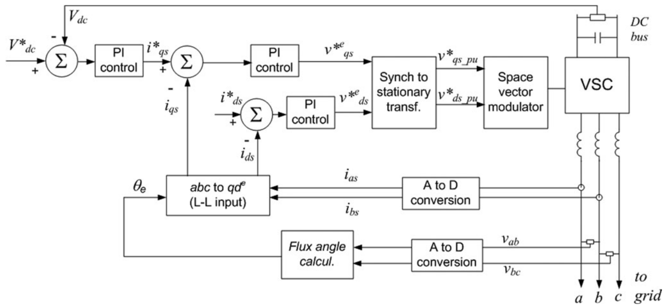

Fig. 6. Grid-side converter control system.

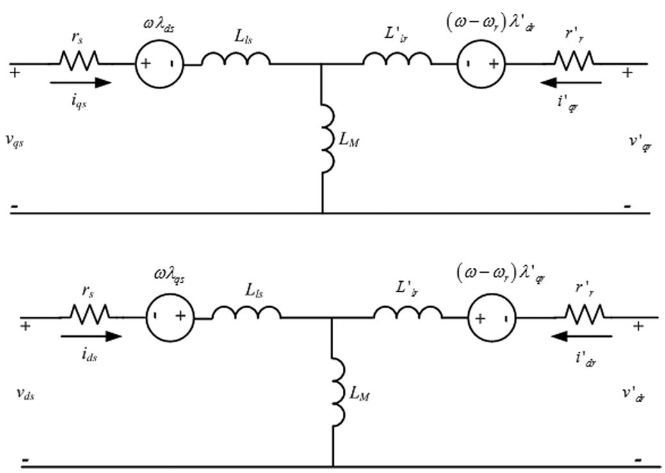

Fig. 7. DFIM equivalent circuits in the *qd* reference frame, using induction machine model 0.

provides a constant dc-bus voltage with bidirectional power flow as described in [9]. The block diagram of the grid-side converter is shown in Fig. 6. All control algorithms are programmed inside the FPGAs in the two SDC2 systems.

V. Machine Model and Simulations

The students are given a MATLAB/Simulink [13] model of the DFIM as part of the class material. The DFIM is modeled using the well-known induction machine equations in the *qd* reference frame. Fig. 7 shows the DFIM equivalent circuits in the q- and d-axes [15].

The differential equations describing the circuits in Fig. 7 are shown in (1) through (4), where ω is the arbitrary reference frame speed and ω_r is the rotor electrical speed. The electromagnetic torque T_e equation is shown in (5) as a function of the currents, where P is the number of poles

$$v_{qs} = r_s i_{qs} + \omega\lambda_{ds} + L_{ls}\frac{di_{qs}}{dt} + L_M\frac{d}{dt}(i_{qs} + i'_{qr}) \quad (1)$$

$$v_{ds} = r_s i_{ds} + \omega\lambda_{qs} + L_{ls}\frac{di_{ds}}{dt} + L_M\frac{d}{dt}(i_{ds} + i'_{dr}) \quad (2)$$

$$v'_{qr} = r'_r i'_{qr} + (\omega - \omega_r)\lambda'_{dr} + L'_{lr}\frac{di'_{qr}}{dt} + L_M\frac{d}{dt}(i'_{qr} + i_{qs}) \quad (3)$$

TABLE I
DFIM Simulation Parameters—0.25 hp Machine Rating

Parameter	r_s	L_{ls}	L_M	r'_r	L'_{lr}	J	B_m
Value	8 Ω	6 mH	0.33 H	32 Ω	6.1 mH	$4\cdot10^{-3}$ Kg m^2	$7.5\cdot10^{3}$ N ·m/(rad/sec)

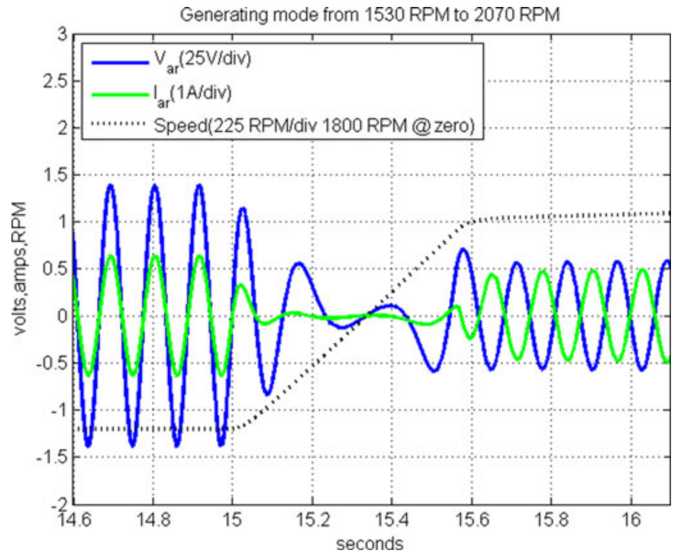

Fig. 8. Simulated rotor current and phase voltage (top) and speed (bottom) in motoring mode.

$$v'_{dr} = r'_r i'_{dr} + (\omega - \omega_r)\lambda'_{qr} + L'_{lr}\frac{di'_{dr}}{dt} + L_M\frac{d}{dt}(i'_{dr} + i_{ds}) \quad (4)$$

$$T_e = \left(\frac{3}{2}\right)\left(\frac{P}{2}\right)L_M(i_{qs}i'_{dr} + i_{ds}i'_{qr}). \quad (5)$$

The DFIM parameters used in the simulations are shown in Table I, where J is the inertia of the rotor and B_m is the damping coefficient. The parameters obtained to match the 0.25 hp, four poles DFIM were used in the remotely controlled laboratory.

The power electronics are idealized in the simulation; therefore, their switching behavior is neglected. Simulation plots are presented in Figs. 8 and 9 for generation and motoring mode of operation, respectively. The pedagogical objective of the simulations is to illustrate that different machine operating modes can be identified by the rotor current frequency and phase angle with respect to the voltage [8], [16]. Fig. 8 shows the simulated rotor current, phase voltage, and speed when the DFIM runs as a generator. This is the case for wind power applications. A change in speed is introduced halfway into the simulation so that the speed changes from subsynchronous to supersynchronous in the same plot. Since the DFIM used in the model and in the laboratory is a four poles machine, synchronous speed is 1800 r/min. From the simulations, the students learn that when the generator operates at supersynchronous speed the rotor current and phase voltage are out of phase (power flows out of the rotor) and they are in phase when the speed is subsynchronous. They also learn that the opposite is true when the machine runs as a

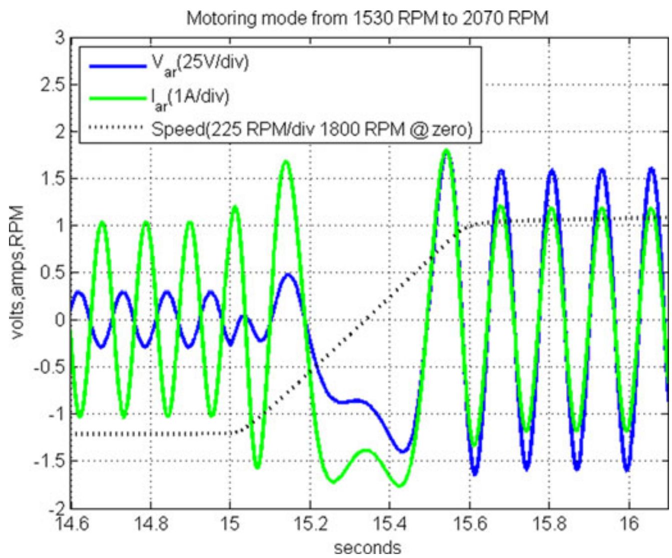

Fig. 9. Simulated rotor current and phase voltage (top) and speed (bottom) in motoring mode.

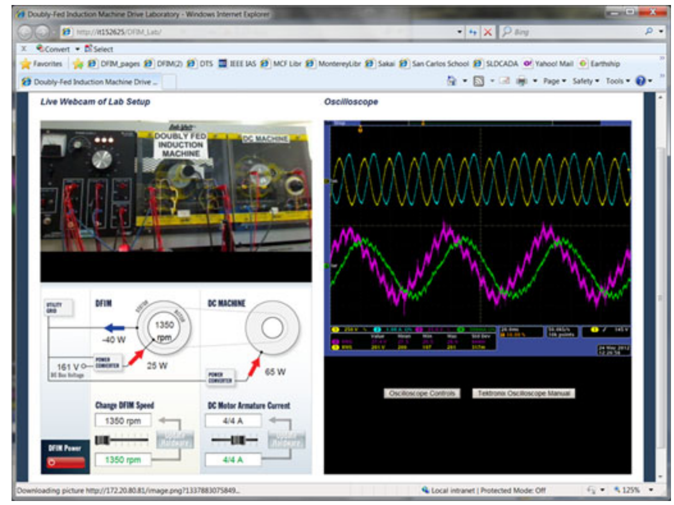

Fig. 10. Screen capture in generating mode, subsynchrounous speed, dc motor armature current 1 A. Oscilloscope plots include stator line-to-line voltage on Channel 1, top, lighter waveform [250 V/div] and current on Channel 2, top, darker waveform [1 A/div] (top). Rotor line-to-line voltage on Channel 3, bottom waveform with larger ripple [25 V/div] and current on Channel 4, bottom waveform with smaller ripple [0.5 A/div].

TABLE II
DFIM Frequency Data From Simulations

	Speed [rpm]	***f_{rotor_mech} [Hz]***	***f_{rotor_elec} [Hz]***
Generator	*2070*	*69*	*-9*
	1530	*51*	*9*
Motor	*2070*	*69*	*-9*
	1530	*51*	*9*

motor, as shown in Fig. 9, where the current and phase voltage in the rotor are in phase at supersynchronous speed and out of phase at subsynchronous speed. These results are reinforced by the experimental measurements that are made during a DL laboratory session, as shown in Section VII.

The relationship between the rotor electrical frequency and the rotor mechanical speed is shown in

$$f_{\text{rotor\_mech}} + f_{\text{rotor\_elec}} = 60 \text{ Hz}. \tag{6}$$

Using (6), the students can measure the mechanical frequency and the electrical frequency from the simulation plots shown in Figs. 8 and 9 and then verify the theory for all modes of operations as shown in Table II.

VI. DL Laboratory Website

A website is set up for the DFIM remote laboratory at the address http://faculty.nps.edu/dl/ec_dfim_lab/index.html. It includes six web pages as follows.

1) introduction;
2) SDC set up description;
3) DFIM description;
4) lab instructions;
5) measurements;
6) report.

The first three pages include information covered in Sections II and IV of this paper. The laboratory instructions of page 4 are reported in the following two sections and refer to the user interface which is shown in Figs. 4, 10, and 13. At the bottom of this page, a "begin lab" button is located. When this button is pushed, a new window will open with the laboratory user interface. This page is password protected and an NPS account is needed to access it.

A. Power Up Instructions as Posted on the DL Laboratory Website

The DL students must make an appointment with the laboratory technician to obtain a 2-h time slot when they can execute the laboratory. Only one user at a given time can operate the hardware remotely. During the selected time slot, the technician turns on the equipment and supervises the hardware for safety. The experimental setup is not enclosed in a secure area, so when the hardware is remotely controlled the laboratory technician must be present so that no resident student can accidentally walk near the hardware. Additionally, the laboratory technician will shut down the equipment if there is a malfunction. The control box and the main power supply are powered up by the laboratory technician. Once power is applied to the experiment and the dc-bus voltage ($V_{\rm dc}$ in Fig. 4) is set to about 160 V, the laboratory is ready to be operated remotely. The voltage applied to the dc bus is displayed in the "dc-bus voltage" field of the web interface (see Figs. 4, 10, and 12).

Push the button labeled "DFIM Power" to turn on the DFIM. The button becomes red when it is pushed and remains red for the entire time the DFIM is ON. Push the button again to turn the DFIM OFF upon the completion of the laboratory exercise.

When the DFIM is ON, its speed can be changed using the slider labeled "Change DFIM Speed." After you move the slider, the button "Update Hardware" will be highlighted blue. Push this button to change the speed to the new one indicated by the slider. The slider "dc motor armature current" operates the same way. Changing the dc motor armature current results in a different load to the DFIM. The drawing above the controls shows the hardware setup and the power readings for DFIM stator and rotor (left-hand side) and dc machine (right-hand side).

Note that the power readings oscillate, so minimum and maximum power readings should be recorded and their average should be used to create the power curves required for the laboratory report.

B. Oscilloscope Setup Information as Posted on the DL Laboratory Website

The oscilloscope is a Tektronix MSO4034 which is web enabled with its own IP address. The link underneath the oscilloscope display provides access to the full-size oscilloscope page where the oscilloscope can be fully controlled and its waveforms can be acquired in different digital formats. The oscilloscope channels are used as follows:

1) channel 1—stator line-to-line voltage $v_{\rm ab}$;
2) channel 2—stator phase a current $i_{\rm as}$;
3) channel 3—inverter output line-to-line voltage $v_{\rm abr}$ (filtered);
4) channel 4—rotor phase a current $i_{\rm ar}$.

The voltages on Channels 1 and 3 are measured with two Tektronix high-voltage differential probes, model P5200. The currents on Channels 2 and 4 are measured by Tektronix current probes TCP305, 50ADC, each connected to a Tektronix current probe amplifier, model TCPA300.

C. Measurements Instructions as Posted on the DL Laboratory Website

The fifth web page includes step-by-step instructions on the type of measurements the students are required to make to complete their laboratory assignment.

1) Check that the dc-bus voltage has been set to 160 V and turn on the DFIM.
2) Collect the data for different dc motor armature currents. The student is given empty tables to fill out. Each table includes columns for: DFIM speed, dc motor power, DFIM stator power, DFIM rotor power, stator and rotor currents ($I_{\rm as}$ and $I_{\rm ar}$). Note that the settings 0, 1/4, and 2/4 result in motoring mode, while settings of 3/4 or higher result in generating mode.
    a) Set the DFIM speed and for each speed value you set:
        i) record the power readings from the user interface. Note that the power readings oscillate, so take min and max readings and average them for your report.
        ii) record the rms stator and rotor currents using the oscilloscope measurements. Use these measurements to estimate the I^2R losses in the machine.
        iii) take a screen capture of your web browser window (as shown in Figs. 4, 10, and 12), including power measurements and oscilloscope, to help answer the questions in the report section.

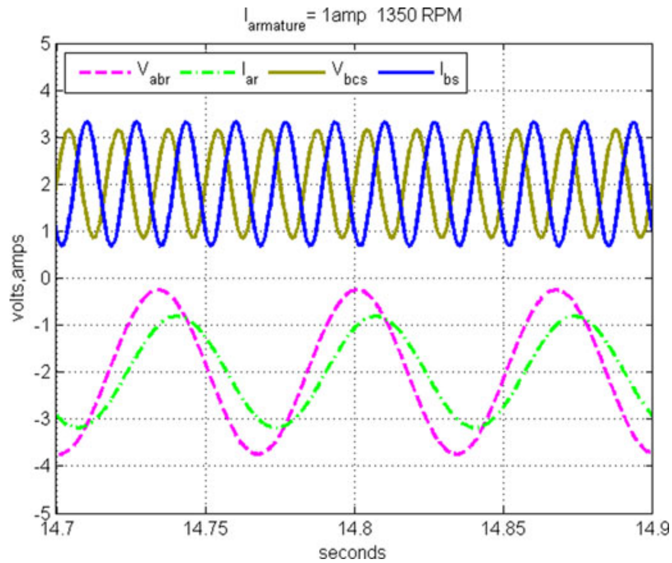

Fig. 11. Simulated plots of stator line-to-line voltage [250 V/div] and current [1 A/div] (top) and rotor line-to-line voltage [25 V/div] and current [0.5 A/div] (bottom) to match the scope plots in Fig. 4. Generating mode, subsynchronous speed.

3) For one speed setting of your choice, compute the rotor power by measuring the rotor current, line–to-line voltage and phase angle. Compare the computed power to the reading in the user interface.
4) Repeat 3 for the stator power.
5) Stop the DFIM after completing the data recording.

VII. DL Laboratory Session

In this section, the experimental results of a DL laboratory session are reported. Each student sets up a 2 h timeframe with the laboratory technician during which the DFIM system is powered ON and ready for use. The student verifies that the power is ON by checking that three lights above the main power switch are ON through the web camera streaming video. The student also checks that the dc-bus voltage reading is around 160 V, as described in the laboratory instructions reported in Section VI. This DL laboratory is set up for a single user and access to the controls window is password protected. While a user is controlling the experiment, if a second user logs in, he/she will be able to view the control window as the first user, except the power button will not be available until the first user has turned off the experiment.

The first goal of the hardware laboratory exercise is to validate the DFIM physics-based model derived in class and used for the simulations as shown in Section V. Figs. 11–14 compare experimental measurements with simulations.

Fig. 10 is a copy of Fig. 4 and shows a screen capture while the DFIM is running as a generator, with dc motor armature current of 1 A (4/4 A in the display) and subsynchronous speed of 1350 r/min. Reading of the power going into the rotor, stator, and dc machine are displayed in the user interface on the left-hand side. On the right-hand side of Fig. 10, the oscilloscope web page is displayed in a miniature version. On the top, the stator

Fig. 12. Web interface screen capture while the DFIM is running in generating mode, supersynchronous speed. Oscilloscope plots include stator line-to-line voltage on Channel 1, top, lighter waveform, [250 V/div] and current on Channel 2, top darker waveform, [1 A/div]. Rotor line-to-line voltage on Channel 3, bottom waveform with larger ripple, [10 V/div] and current on Channel 4, bottom waveform with smaller ripple [0.5 A/div].

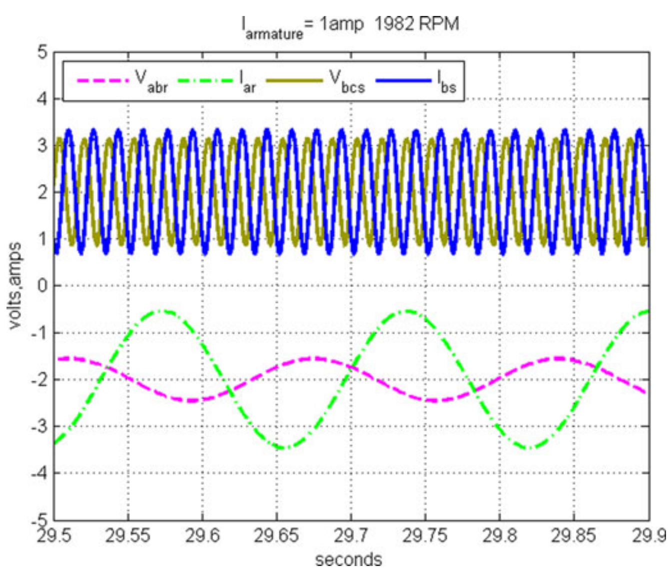

Fig. 13. Simulated plots of stator line-to-line voltage [250 V/div] and current [1 A/div] (top) and rotor line-to-line voltage [10 V/div] and current [0.5 A/div] (bottom) to match the scope plots in Fig. 13. Generating mode, supersynchronous speed.

line-to-line voltage (Channel 1) and phase current (Channel 2) are displayed. On the bottom, the filtered line-to-line voltage at the output of the inverter (Channel 3) and the rotor phase current (Channel 4) are plotted. Fig. 11 shows the simulation results created with the same scaling factors as the experimental waveforms in Fig. 10. We can observe a good match for current and voltages amplitudes and phase angles; however, the simulation waveforms are ideally smooth and do not present the ripple that can be observed experimentally. The lack of high frequency noise in the simulations is due to the fact the power converter switching is not included in the DFIM model. The low frequency noise in the experimental rotor waveforms (bottom of

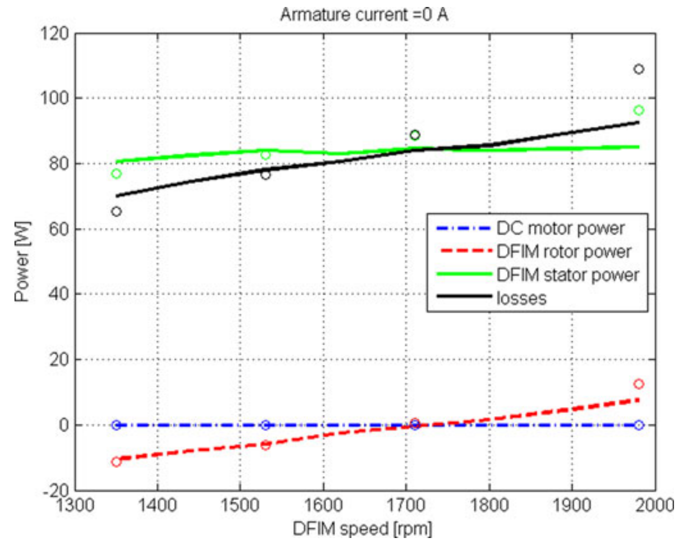

Fig. 14. Experimental data and simulated data (circles) plotted versus speed. Motoring mode of operation.

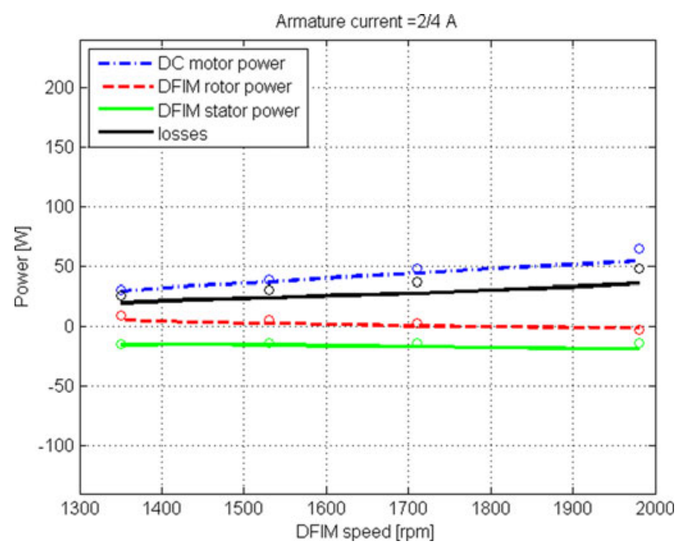

Fig. 15. Experimental data and simulated data (circles) plotted versus speed. Generating mode of operation with dc motor armature current 0.5 A.

oscilloscope) is due to distortion in grid voltage, which is also not included in the simulations [17]. As described in Section IV, the Simulink model used in class is limited to the electric machine. Figs. 12 and 13 compare experimental measurements and simulations for supersynchronous speed.

In addition to waveform acquisition with the oscilloscope, the DL laboratory real-time experience includes audio and video feedback; the remote students can hear the DFIM emitting different sounds at different speeds and loads and see the hardware in the laboratory.

After the students follow all the steps reported in Section V-C, they create the plots shown in Figs. 14–17. The solid lines are plotted using the experimental data, while the circles are simulation results. The "losses" lines in Fig. 14 through Fig. 17 represent the sum of the power into the three electrical input ports of the systems, as shown in (7). Note that the field current

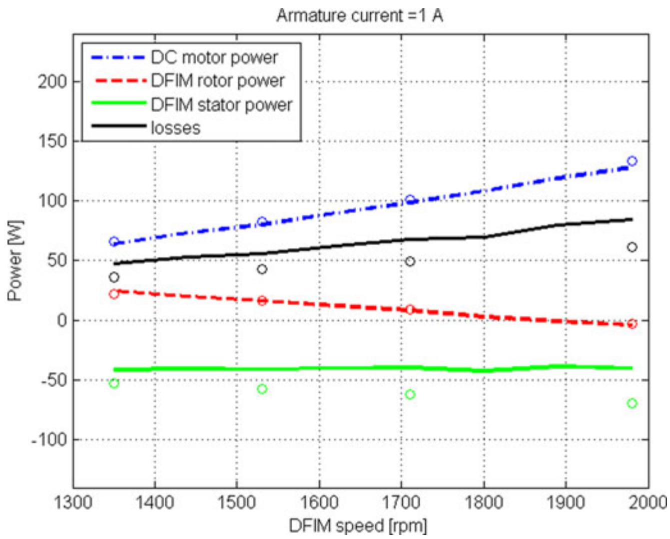

Fig. 16. Experimental data and simulated data (circles) plotted versus speed. Generating mode of operation with dc motor armature current 1 A.

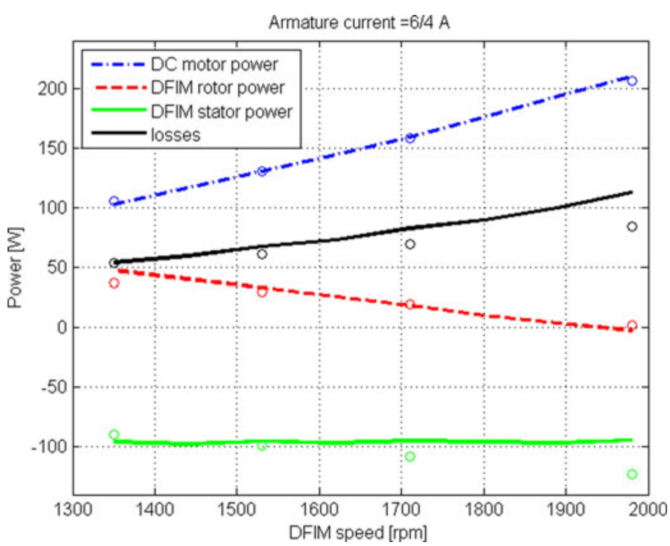

Fig. 17. Experimental data and simulated data (circles) plotted versus speed. Generating mode of operation with dc motor armature current 1.5 A.

losses in the dc machine are not included

$$\text{losses} = P_{\text{DFIM\_rotor}} + P_{\text{DFIM\_stator}} + P_{\text{DCmotor\_armature}}. \tag{7}$$

The comparison of experimental and simulated data show that the linear model of the DFIM presented in Section V is reasonably accurate, but not perfect.

VIII. Students' Feedback

During the spring quarter of 2012, the DFIM laboratory was assigned to the advanced electric machinery (EC4130) students at NPS for the first time. The students were resident but they used the remote interface to operate the laboratory. They were asked to complete a brief survey after completing the laboratory assignment. Nine students completed the survey and the responses are reported in Table III. The responses show that the students generally liked the laboratory experience with Internet access. Since this was the first time, the laboratory was assigned several comments from the students helped improve the laboratory instructions on the DL laboratory website.

TABLE III
Student Survey Results

Question 1. The remotely controlled laboratory provides an authentic and realistic experience in support of the class material.					
1 Strongly disagree	2 Disagree	3 No Strong opinion	4 Agree	5 Strongly agree	**Rating Average**
0.0% (0)	11.1% (1)	0.0% (0)	**77.8% (7)**	11.1% (1)	**3.89**
Question 2. The online materials provide sufficient instructions and resources to complete the laboratory.					
1 Strongly disagree	2 Disagree	3 No Strong opinion	4 Agree	5 Strongly agree	**Rating Average**
0.0% (0)	22.2% (2)	0.0% (0)	**77.8% (7)**	0.0% (0)	**3.56**
Question 3. Overall, the remotely controlled laboratory provides an equivalent learning experience when compared to a traditional laboratory experience.					
1 Strongly disagree	2 Disagree	3 No Strong opinion	4 Agree	5 Strongly agree	**Rating Average**
0.0% (0)	22.2% (2)	11.1% (1)	**66.7% (6)**	11.1% (1)	**4.00**

The students that selected "strongly disagree" explained that they did not like the remotely controlled laboratory as much as they like traditional hands-on laboratories on campus. However, they admitted that for DL students who cannot be on campus, the remotely controlled laboratory is a good alternative to simulations.

The oscilloscope control page was generally considered hard to use, so future work includes plotting the waveforms using the data from the FPGA in a user-friendly manner.

IX. Conclusion

A new DL laboratory featuring a DFIM drive has been successfully designed and demonstrated to supply remote students with the hardware experience which is typically available only to resident students. The laboratory is accessible via a standard web browser and the DL students only need Internet access. The students do not need administrator rights because the DL laboratory operation does not require software installation or security setting changes. This feature is important for students, like NPS Department of Defense civilian DL students, who use their employer's computers for all class work. In most cases, they do not have administrator rights.

The logistic and pedagogical challenges of delivering the laboratory experience to DL students are addressed and their solutions highlighted. Particularly, an innovative system, the SDC2, was designed to include the power conversion elements, sensors, and all necessary components to control the DFIM and effectively communicate with a web server via a USB interface. The DL laboratory offers a meaningful experience to remote students because they can hear, see, and interact with the hardware. They use an oscilloscope to measure currents and voltages and acquire data to build confidence that the simulations are correct.

Students' feedback was collected and it is positive. Future work will include increasing the involvement of the student in the drive's control system design, which is presently not possible.

ACKNOWLEDGMENT

The authors gratefully acknowledge the Naval Postgraduate School's Center for Educational Design, Development, and Distribution for its support and especially T. Mastre, the Director, Philip McCullick for programming the graphic user interface and Sherrill Meaney for the website layout and students' survey.

REFERENCES

[1] P. Bauer, V. Fedak, V. Hajek, and I. Lampropoulos, "Survey of distance laboratories in power electronics," in *Proc. IEEE Power Electron. Spec. Conf.*, 2008, pp. 430–436.

[2] F. J. Rodriguez, C. Giron, E. J. Bueno, A. Hernandez, S. Cobreces, and P. Martin, "Remote laboratory for experimentation with multilevel power converters," *IEEE Trans. Ind. Electron.*, vol. 56, no. 7, pp. 2450–2463, Jul. 2009.

[3] G. Oriti, D. Zulaica, A. L. Julian, and R. Cristi, "Hardware laboratories for power electronics and motor drives distance learning courses," in *Proc. IEEE 2nd Energy Convers. Conf. Expo.*, Atlanta, GA, USA, Sep. 2010, pp. 2229–2236.

[4] E. Ernest, R. Sztylka, B. Ufnalski, and W. Koczara, "Methods in teaching modern AC drives: Inverter-fed motor system with internet-based remote control panel," in *Proc. Power Electron. Motion Control Conf.*, 2006, pp. 2130–2133.

[5] R. Marques, J. Rocha, S. Rafael, and J. F. Martins, "Design and implementation of a reconfigurable remote laboratory, using oscilloscope/PLC network for WWW access," *IEEE Trans. Ind. Electron.*, vol. 55, no. 6, pp. 2425–2432, Jun. 2008.

[6] V. J. Harward, J. A. del Alamo, S. R. Lerman, P. H. Bailey, J. Carpenter, K. DeLong, C. Felknor, J. Hardison, B. Harrison, I. Jabbour, P. D. Long, T. Mao, L. Naamani, J. Northridge, M. Schulz, D. Talavera, C. Varadharajan, S. Wang, K. Yehia, R. Zbib, and D. Zych, "The iLab shared architecture: A web services infrastructure to build communities of internet accessible laboratories," *Proc. IEEE*, vol. 96, no. 6, pp. 931–950, Jun. 2008.

[7] W. G. Hurley and C. K. Lee, "Development, implementation, and assessment of a web-based power electronics laboratory," *IEEE Trans. Educ.*, vol. 48, no. 4, pp. 567–573, Nov. 2005.

[8] S. Muller, M. Deicke, and R. W. De Doncker, "Doubly fed induction generator systems for wind turbines," *IEEE Ind. Appl. Mag.*, vol. 8, no. 3, pp. 26–33, May/Jun. 2002.

[9] R. Pena, J. C. Clare, and G. M. Asher, "Doubly fed induction generator using back-to-back PWM converters and its application to variable speed wind-energy generation," *IEE Proc.-Electr. Power Appl.*, vol. 143, no. 3, pp. 231–241, May 1996.

[10] F. W. Fuchs, J. Dannehl, R. Lohde, V. Dinkhauser, S. Jensen, A. Knop, K. Rothenhagen, S. Thomsen, and C. Wessels, "Research laboratory for power electronic generator systems in wind turbines comprising converters, generators, interaction and grid interaction," in *Proc. 13th Eur. Conf. Power Electron. Appl.*, 2009, pp. 1–15.

[11] J. R. Arribas, C. Veganzones, F. Blázquez, C. A. Platero, D. Ramírez, S. Martínez, J. A. Sánchez, and N. H. Martínez, "Computer-based simulation and scaled laboratory bench system for the teaching and training of engineers on the control of doubly fed induction wind generators," *IEEE Trans. Power Electron.*, vol. 26, no. 3, pp. 1534–1543, Aug. 2011.

[12] Xilinx "Avnet Virtex-4 LC development board," (2013). [Online]. Available: http://www.xilinx.com/products/devkits/DS-KIT-4VLX25LC.htm

[13] (2013). [Online]. Available: http://www.mathworks.com/

[14] G. Oriti and A. L. Julian, "Three phase VSI with FPGA based multisampled space vector modulation," *IEEE Trans. Ind. Appl.*, vol. 47, no. 4, pp. 1813–1820, Jul./Aug. 2011.

[15] P. C. Krause, O. Wasynczuk, and S. D. Sudhoff, *Analysis of Electric Machinery and Drive Systems*. Piscataway, NJ, USA: IEEE Press, 2002.

[16] G. W. Edwards, "Wind turbine power generation emulation via doubly fed induction generator control," Master's thesis, Naval Postgraduate School, Electr. Comput. Eng. Dept., Monterey, CA, USA, Dec. 2009.

[17] C. Liu, F. Blaabjerg, W. Chen, and D. Xu, "Stator current harmonic control with resonant controller for doubly fed induction generator," *IEEE Trans. Power Electron.*, vol. 27, no. 7, pp. 3207–3220, Jul. 2012.

Giovanna Oriti (S'94–M'97–SM'04) received the Laurea (with Hons.) and Ph.D. degrees in electrical engineering from the University of Catania, Catania, Italy, in 1993 and 1997, respectively.

She was a Research Intern at the University of Wisconsin, Madison, for two years. After graduation she joined United Technology Research Center where she developed innovative power converter topologies and control. In 2000, she launched her own consulting business developing physics-based models of power converters and drives for electromagnetic interference analysis, stability analysis and development of control algorithms. In April 2008, she joined the faculty of the Electrical and Computer Engineering (ECE) Department of the Naval Postgraduate School, where she is now Associate Professor. She is involved in electric ship systems and energy management research activities. She is leading the development of remotely controlled hardware laboratories for resident and distance learning students.

Dr. Oriti holds one U.S. Patent and has coauthored more than 30 papers published in IEEE TRANSACTIONS or IEEE conference proceedings. She currently serves as past chair of the Industrial Power Conversion System Department of the IEEE Industry Application Society (IAS). She was the recipient of the 2002 IEEE IAS Outstanding Young Member Award. In 2012, she received the NPS ECE Service Award in recognition of her contribution to the development of the new NPS EE Energy curriculum.

Alexander L. Julian (S'91–M'98) received the B.S.E.E. and M.S.E.E. degrees from the University of Missouri, Columbia, MO, USA, in 1991 and 1992, respectively, and the Ph.D. degree in electrical engineering from the University of Wisconsin, Madison, WI, USA, in 1998.

In March 2004, he joined the Faculty of the Naval Postgraduate School as Assistant Professor at the ECE Department of the Graduate School of Engineering and Applied Sciences (GSEAS). Before joining NPS he contributed to shipboard electronic designs and research for many years as a consultant to Navy vendors by designing, modeling and prototyping power electronics and motion control systems for many Navy applications. His research interests include solid state power converter design and control, electromagnetic interference, reliability analysis, and stability analysis for distributed power systems.

Dr. Julian holds 4 U.S. patents and has coauthored more than 30 papers in IEEE TRANSACTIONS or IEEE conference proceedings. He is a Reviewer for the IEEE TRANSACTIONS IN INDUSTRY APPLICATIONS, the IEEE TRANSACTIONS ON POWER ELECTRONICS, and the IEEE TRANSACTIONS ON CONTROL SYSTEMS.

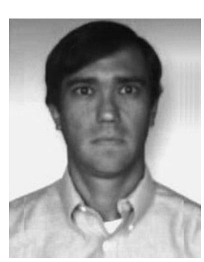

Daniel P. Zulaica (M'11) received the B.S. degree in physics from the University of Texas at Arlington, in 1981. He has contributed to research and education projects at the U.S. Naval Postgraduate School in two full-time segments as well as a few years as a part-time consultant.

His interests include FPGA, VLSI, and image processing development and computer programming with simulations, as well as radar research. He also enjoys contemplating the mysteries of life and the universe.